Journal of Applied Fluid Mechanics, Vol. 11, No. 6, pp. 1717-1726, 2018.
Available online at www.jafmonline.net, ISSN 1735-3572, EISSN 1735-3645.
DOI: 10.29252/jafm.11.06.28566

Self-Similar Motion of Strong Converging Cylindrical and Spherical Shock Waves in Non-Ideal Stellar Medium

D. Narsimhulu, A. Ramu† and D. Kumar Satpathi

Department of Mathematics, Birla Institute of Technology and Science – Pilani, Hyderabad Campus, Shameerpet, Hyderabad,Telangana, 500078, India

†*Corresponding Author Email: aramu@hyderabad.bits-pilani.ac.in*

(Received November 6, 2017; accepted June 19, 2018)

ABSTRACT

A theoretical model for strong converging cylindrical and spherical shock waves in non-ideal gas characterized by the equation of state (EOS) of the Mie-Gruneisen type is investigated. The governing equations of unsteady one dimensional compressible flow including monochromatic radiation in Eulerian hydrodynamics are considered. These equations are reduced to a system of ordinary differential equations (ODEs) using similarity transformations. Shock is assumed to be strong and propagating into a medium according to a power law. In the present work, two different equations of state (EOS) of Mie-Gruneisen type have been considered and the cylindrical and spherical cases are worked out in detail. The complete set of governing equations is formulated as finite difference problem and solved numerically using MATLAB. The numerical technique applied in this paper provides a global solution to the problem for the flow variables, the similarity exponent α for different Gruneisen parameters. It is observed that increase in measure of shock strength $\beta\left(\frac{\rho}{\rho_0}\right)$ has effect on the shock front. The velocity and pressure behind the shock front increases quickly in the presence of the monochromatic radiation and decreases gradually. A comparison between the results obtained for non-ideal and perfect gas in the presence of monochromatic radiation has been illustrated graphically.

Keywords: Shock waves; Radiation hydrodynamics; Finite difference methods; Rankine-Hugoniot jump relations; Mie-Gruneisen EOS; Numerical solution.

NOMENCLATURE

A°	proportionality constant	α	similarity exponent
b	non-idealness parameter	β	shock density ratio
$\frac{D}{Dt}$	substantial derivative	γ	specific heat ratio
e	specific internal energy	λ	similarity variable
j	flux of monochromatic radiation	π	non-dimensional pressure
K	absorption coefficient	ρ	density of gas
r	radial coordinate	ρ_0	density of unperturbed medium
$R_s(t)$	radius of the shock wave	σ	material property
t	time coordinate	ψ	non-dimensional radiation flux
u	velocity of gas particles	$\Gamma(\rho/\rho_0)$	gruneisen coefficient
v	non-dimensional velocity	Γ_0	gruneisen parameter
W	scale of velocity	Ω	geometrical index

1. INTRODUCTION

Shock processes occurs naturally in various processes which are related to hydrodynamics, astrophysical situations such as supernova explosions, photo-ionized gas, stellar winds, interstellar gas etc. They are considered to be discontinuities in mathematical point of view but shock wave is not a true physical discontinuity. The study of converging spherical and cylindrical shock waves in non-ideal stellar atmosphere under the action of monochromatic radiation is of importance because of its applications in the areas of nuclear engineering, cavitation, astrophysics, radioactively driven outflows, stellar convection, and inertial confinement fusion. The theory of radiation hydrodynamics plays an important role in studying phenomena in plasma physics. These shock fronts have a more complex structure than ordinary hydrodynamical shocks. In recent years, the problems of high-temperature gas dynamics have attracted much attention. The high temperatures generated in gases by shock waves give rise to physical and chemical phenomena such as molecular vibrational excitation, dissociation, ionization, chemical reactions, and inherently related radiation. In continuum regime, these processes start from the wave front, so that generally the gaseous media behind the shock waves may be in thermodynamic and chemical non-equilibrium state. In the flow field of a gas at very high temperatures, the gas may be ionized and the radiation transfer is important. In classical gas dynamics the transfer of radiation is usually neglected, however, when the temperature of the gas is high, radiation can be considered as an important mode of energy transport. The gas temperature behind such a shock could depart strongly from that predicted by the standard Rankine-Hugoniot law.

Gail *et al*. (1990) discussed applications to weak and strong shocks in a stellar atmosphere due to a shock wave trains. The effect of non-linear interactions of one dimensional adiabatic or isothermal hydrodynamic shock waves in the solar atmosphere have been studied by Fleck and Schmitz (1993). Barnwal and Srivastava (1983) have investigated the general Rankine-Hugoniot jump relations for a 3-dimensional shock in dusty gas in the presence of radiation. Neglecting the radiation pressure and energy, they have presented similarity solutions for a stellar line explosion into a non-uniform self-gravitating medium with effect of magnetic radiation flux. Several authors (Elliott 1960; Helliwell 1969; Nicastro 1970; Ghoniem 1993; Gretler and Steiner 1993; Sedov studied the shock wave problem with thermal radiation by similarity method (Sedov 1982) in perfect gas. Marshak (1958) studied the effect of radiation on the shock propagation by introducing the radiation diffusion approximation. Elliott (1960) discussed the conditions leading to self-similarity with a specified functional form of the mean free-path of radiation and obtained a solution for self-similar explosion. Hirschler and Gretler (2002) studied similarity solutions of converging spherical shock wave with radiation effect by assuming medium to be optically thick. Khudyakov (1983) discussed the self-similar problem of motion of a gas under the action of monochromatic radiation.

In recent times considerable study for the self-similar solutions in the process occurring under the action of monochromatic radiation of gaseous substances in the stellar regions has gained importance. Several problems relating to shock wave propagation in perfect gas and non-ideal gas with radiative and magneto hydrodynamic effects have been studied by Zedan (2002), Leygnac *et al*. (2006), Sampaio (2013), Taylor and Ryan (2013). The assumption that the medium in an astrophysical environment to follow the ideal gas may not be true in reality and it is necessary to analyze the gas dynamic processes in a non-ideal medium with monochromatic radiation. In the present problem a model to determine the self-similar solutions for converging spherical and cylindrical strong shock waves in stellar atmosphere under the action of monochromatic radiation in non-uniform stellar interiors with constant intensity on a unit area with the assumption that the medium of propagation to be non-ideal gas is presented. Shock is assumed to be strong and obeys a power law. It is assumed that the radiation flux moves through the gas with constant intensity on a unit area of the shock wave propagation in a direction opposite to the radiation flux. The medium of flow is assumed to be obeying the equation of state of Mie-Grüneisen type i.e., Royce EOS (Ramu and Rangarao 1993). The perfect gas EOS results too are obtained from Royce EOS, and were found to match very closely with the literature.

2. FORMULATION OF THE PROBLEM

The basic equations for one-dimensional unsteady motion of cylindrical and spherical strong converging shock waves into the radiation hydrodynamic regime with the medium neglecting viscosity, heat conduction, and magnetic field characterized by the equation of state (EOS) of Mie-Grüneisen type can be written in Eulerian form (Gretler and Steiner 1993; Narsimhulu *et al*. 2013)

$$\frac{D\rho}{Dt} + \rho(\nabla . u) + (\Omega - 1)\frac{\rho u}{r} = 0 \tag{1}$$

$$\frac{Du}{Dt} + \frac{1}{\rho}\nabla p = 0 \tag{2}$$

$$\frac{De}{Dt} - \frac{p}{\rho}\frac{D}{Dt}\left[ln\left(\frac{\rho}{\rho_0}\right)\right] + \frac{1}{\rho r}\nabla(jr) = 0 \tag{3}$$

$$\nabla j = Kj \tag{4}$$

where $\frac{D}{Dt} = \frac{\partial}{\partial t} + (u.\nabla)$ is the substantial derivative, which is the sum of local and convective derivatives. $\Omega = 2, 3$ denote the geometrical index for cylindrical and spherical cases of the shock waves respectively and ρ, ρ_0, u, p, e, j, K denote the density of gas, density of unperturbed medium, velocity of gas particles, pressure, specific internal energy per unit mass of volume, the flux of monochromatic radiation per unit area at radial

distance r from the axis at time t and absorption coefficient respectively.

The equation of state under equilibrium condition is of Mie-Grüneisen type (Ramu and Ranga Rao 1993; Ramu *et al*. 2014; Narsimhulu *et al*. 2016)

$$e = \frac{p}{\rho\Gamma(\rho/\rho_0)} \tag{5}$$

where $\Gamma(\rho/\rho_0)$ is the Mie-Grüneisen coefficient.

The above governing Eqs. (1)-(4) can be written in matrix equation as follows

$$F_t + AF_r + B = 0 \tag{6}$$

where F, A and B are given by

$$F = \begin{bmatrix}\rho\\ u\\ e\\ 0\end{bmatrix}, A = \begin{bmatrix}u & \rho & 0 & 0\\ 0 & u & 1/\rho & 1/\rho\\ 0 & p/\rho & u & 1/\rho\\ 0 & 0 & 0 & 1\end{bmatrix}, \text{and}$$

$$B = \begin{bmatrix}\frac{(\Omega-1)\rho u}{r}\\ 0\\ \frac{(\Omega-1)pu}{\rho r}+\frac{j}{\rho r}\\ -Kj\end{bmatrix}$$

F_t and F_r are partial derivatives with respect to time t and spacial coordinate r. The absorption coefficient K is considered to vary as Khudyakov (1983)

$$K = K_0\rho^n p^m j^q r^s t^l \tag{7}$$

where the numbers n, m, q, s, l are rational exponents and

$$[K_0] = M^{-n-m-q}L^{3n+m-s}T^{2m+3q-l} \tag{8}$$

In the present problem, the quantities p_0, ρ_0, j_0, and K_0 are dimensional constants, in which p_0, ρ_0, and j_0 are dependent given by

$$j_0 = [p_0]^{3/2}[\rho_0]^{-1/2} \tag{9}$$

The radiation absorption coefficient K depends on dimensions of j_0, ρ_0, which is equivalent $s + l = -1$.

2.1 Rankine-Hugoniot Relations

The jump conditions across a shock wave propagating in an electrically conducting and radiating gas are given by (Ramu *et al*. 2014; Narsimhulu *et al*. 2016)

$$[(u-W)\rho]_1^2 = 0 \tag{10}$$

$$[p+\rho u^2]_1^2 = 0 \tag{11}$$

$$\left[e+\frac{p}{\rho}+\frac{1}{2}(u-W)^2\right]_1^2 = 0 \tag{12}$$

$$[j]_1^2 = 0 \tag{13}$$

where the symbol $[...]_1^2$ represents the difference between the values of ahead upstream and behind downstream regions across shock wave respectively and W represents the scale of velocity. We assume that shock is propagating into a non-ideal stellar medium at rest with gas density varying as the power law given by (Ramu and Rangarao 1993)

$$R_s(t) = \text{Å}(-t)^{\alpha} \tag{14}$$

where the function $R_s(t)$ is the time-dependent radius of the shock wave, Å is proportionality constant and α is an unknown similarity exponent. It is assumed that the radiation pressure and radiation energy are very small in comparison to the material pressure and energy, hence neglected. For the case of strong shocks, the upstream medium can be approximated as a cold fluid ($T\sim0$). The upstream pressure can therefore be neglected in comparison to other quantities appearing in the Rankine-Hugoniot jump conditions (10)-(13). Setting $p_1 = 0$, $u_1 = 0$ in the above equations, Rankine-Hugoniot jump conditions become

$$\frac{\rho_2}{\rho_1} = \beta^{-1} \tag{15}$$

$$u_2 = (1-\beta)W \tag{16}$$

$$p_2 = \rho_1(1-\beta)W^2 \tag{17}$$

$$e_2 = \frac{1}{2}(1-\beta)^2W^2 \tag{18}$$

$$j_1 = j_0 \tag{19}$$

where β is the shock density ratio and its magnitude is dependent on the equation of state (EOS) and $W = \frac{dR_s}{dt}$. The effect of ionization, dissociation, and the interaction with radiation become important on the Rankine-Hugoniot jump relations when the shock is strong. Along with the strong shock relations (15)-(19) and the EOS (5), we get

$$(\beta-1)\Gamma(\beta) = 2 \tag{20}$$

2.2 One-dimensional Self-similar Motion

The basic equations are non-dimensionalized by using dimensionless functions of the similarity variable λ (Zeldovich and Raizer 1967; Ramu and Ranga Rao 1993; Ramu *et al*. 2014) are

$$\rho = \rho_0 g(\lambda) \tag{21. a}$$

$$u = v(\lambda)W \tag{21. b}$$

$$p = \rho_0 W^2\pi(\lambda) \tag{21. c}$$

$$j = j_0\psi(\lambda) \tag{21. d}$$

where g, v, π, and ψ are non-dimensional density, velocity, pressure, and radiation flux of similarity variable λ respectively. For computational convenience, we consider another set of transformations along with the above transformations as

$$g(\lambda) = G(\lambda) \tag{22. a}$$

$$v(\lambda) = \frac{\lambda}{\alpha}U(\lambda) \tag{22. b}$$

$$\pi(\lambda) = \frac{\lambda^2}{\alpha^2}P(\lambda) \tag{22. c}$$

$$\psi(\lambda) = J(\lambda) \tag{22. d}$$

and $Y(\lambda) = P(\lambda)/G(\lambda)$, where G, U, P, and J are

new reduced density, velocity, pressure, and radiation flux functions in terms of similarity variable λ respectively.

Applying the similarity transformations the equations of motion take the form

$$\frac{(U-\alpha)}{G}\frac{dG}{d\lambda}+\frac{dU}{d\lambda}+\frac{\Omega U}{\lambda}=0 \tag{23}$$

$$\frac{1}{G}\frac{dG}{d\lambda}+(U-\alpha)\frac{dU}{d\lambda}+\frac{dY}{d\lambda}+$$

$$\frac{1}{\lambda}[2Y+U(U-1)]=0 \tag{24}$$

$$\frac{Y\Phi(G)}{G}\frac{dG}{d\lambda}+\frac{dY}{d\lambda}+\left[\frac{\frac{2(U-1)Y}{\lambda(U-\alpha)}+}{\frac{\alpha^3\Gamma(G)(U-1)YJ}{(U-\alpha)^2R^3\lambda^4\rho_0G(J'+1)}}\right]=0 \tag{25}$$

$$\frac{dJ}{d\lambda}-\alpha\lambda^sG^nP^mJ^{q+1}=0 \tag{26}$$

where

$$\Phi(G)=-\Gamma(G)-\frac{G}{\Gamma(G)}\frac{d\Gamma(G)}{dG} \quad \text{and}$$

$$1-\phi(G)=\sigma \tag{27}$$

where σ is the material property. At the shock front, the boundary conditions (15)-(19) are transformed into the following form

$$G(1)=\frac{1}{\beta} \tag{28}$$

$$U(1)=(1-\beta)\alpha \tag{29}$$

$$P(1)=\beta(1-\beta)\alpha^2 \tag{30}$$

$$J(1)=1 \tag{31}$$

3. NUMERICAL SOLUTION

3.1 Finite Difference Formulation

An explicit finite difference method is employed in solving system of Eqs. (23)-(26). The solution domain is discretized by a one-dimensional set of discrete grid points, with the grid points equally spaced having uniform spacing Δλ.

The finite difference approximations of the transformed system of Eqs. (23)-(26) are given by

$$\frac{dG}{d\lambda}=\frac{G_{i+1}-G_i}{\Delta\lambda} \tag{32}$$

$$\frac{dU}{d\lambda}=\frac{U_{i+1}-U_i}{\Delta\lambda} \tag{33}$$

$$\frac{dY}{d\lambda}=\frac{Y_{i+1}-Y_i}{\Delta\lambda} \tag{34}$$

$$\frac{dJ}{d\lambda}=\frac{J_{i+1}-J_i}{\Delta\lambda} \tag{35}$$

Substituting Eqs. (32)-(35) into Eqs. (23)-(26) the resulting system of equations can be written in the following matrix form,

$$[C_i][X_{i+1}]=[D_i] \tag{36}$$

where $[C_i]$, $[X_{i+1}]$ and $[D_i]$ are 4x4, 4x1and 4x1 matrices respectively.

$$[C_i]=\begin{bmatrix}(U_i-\alpha) & G_i & 0 & 0\\ 1 & G_i(U_i-\alpha) & G_i & 0\\ Y_i\Phi(G_i)/G_i & 0 & 1 & 0\\ 0 & 0 & 0 & 1\end{bmatrix} \tag{37}$$

$$[X_{i+1}]=[G_{i+1}\quad U_{i+1}\quad Y_{i+1}\quad J_{i+1}]^T \tag{38}$$

and

$$[D_i]=\begin{bmatrix}\left(2-\frac{h\Omega}{\lambda_i}\right)G_iU_i-\alpha G_i\\ \left(1-\frac{2h}{\lambda_i}\right)G_iY_i-\frac{h}{\lambda_i}G_iU_i(U_i-1)+G_iU_i(U_i-\alpha)+G_i\\ \frac{-h}{\lambda_i}Y_i\left\{\frac{\frac{2(U_i-1)}{(U_i-\alpha)}+}{\frac{\alpha^3J_i(U_i-1)\Gamma(G_i)}{(U_i-\alpha)^3R^3{\lambda_i}^3\rho_0G_i(J_i'+1)}}\right\}+Y_i\{1+\Phi(G_i)\}\\ h\alpha{\lambda_i}^s{G_i}^n{P_i}^m{J_i}^{q+1}+J_i\end{bmatrix} \tag{39}$$

Crout's reduction technique (Samuel D. Conte and Carl de Boor 1981) is employed to evaluate the flow parameters such as density (G_{i+1}), velocity (U_{i+1}), pressure (Y_{i+1}) and radiation flux (J_{i+1}) where

$$G_{i+1}=\frac{(U_i-\alpha)(D_{11})^{(i)}-(D_{21})^{(i)}+G_i(D_{31})^{(i)}}{[(U_i-\alpha)^2+Y_i\Phi(G_i)-1]} \tag{40}$$

$$Y_{i+1}=\frac{\{(D_{21})^{(i)}-(U_i-\alpha)(D_{11})^{(i)}\}Y_i\Phi(G_i)+}{\frac{G_i\{(U_i-\alpha)^2-1\}(D_{31})^{(i)}}{[(U_i-\alpha)^2+Y_i\Phi(G_i)-1]G_i}} \tag{41}$$

$$U_{i+1}=\frac{\{Y_i\Phi(G_i)-1\}(D_{11})^{(i)}+(U_i-\alpha)(D_{21})^{(i)}-}{\frac{G_i(U_i-\alpha)(D_{31})^{(i)}}{[(U_i-\alpha)^2+Y_i\Phi(G_i)-1]G_i}} \tag{42}$$

$$J_{i+1}=(D_{41})^{(i)} \tag{43}$$

where the superscript i refers to the location in the discretizing continuous solution domain and it is a positive integer. Numerical solution of system of Eqs. (40)-(43) along with boundary conditions (28)-(31) are obtained for a step size of $h=10^{-4}$.

3.2 Evaluation of $\beta(\rho/\rho_0)$ the Measure of Shock Strength

Considering the EOS of Mie-Grüneisen type (Ramu and Ranga Rao 1993):

The Royce EOS defined by

$$\Gamma(G)=\Gamma_0-b\left(1-\frac{1}{G}\right) \tag{44}$$

where b is constant such that $b>0$ and Γ_0 is the non-idealness parameter.

Using Eq. (44) in Eq. (20), gives a quadratic expression in terms of β and it can be written as

$$Z(\beta)\equiv(\Gamma_0-b)\beta^2+(2b-\Gamma_0-2)\beta-b=0 \tag{45}$$

The Eq. (44) reduces to perfect gas EOS when $\Gamma_0=(\gamma-1)$, $b=0$ and along with Eq. (5) which is

$$p(\rho,e)=\rho e(\gamma-1) \tag{46}$$

the measure of shock strength β defined by the following relation

$$\beta=\frac{\gamma+1}{\gamma-1}, \text{ provided } \beta\neq 0 \tag{47}$$

Positive roots are only considered in the subsequent

computation. The solution curves of the polynomial $Z(\beta)$ for two different values of non-idealness parameter Γ_0 are shown in Fig. 1.

The values of measure of the shock strength β, similarity exponent α along with the known values of non-idealness parameter Γ_0, adiabatic index γ, and constant parameter b are presented in Tables 1 and 2 for Royce and perfect gas EOS respectively.

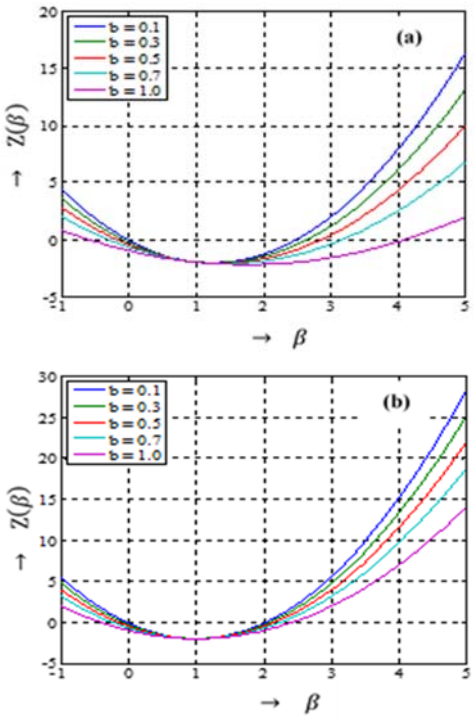

Fig. 1. Graphical approach of $Z(\beta)$ in the case of Royce EOS; (a) $\Gamma_0 = 1.4$ and (b)

Table 1 Selected values of α for Royce EOS

b	$\Gamma_0 = 1.4$		$\Gamma_0 = 2.0$	
	β	α	β	α
0.1	2.49240	0.43013	2.02598	0.45569
0.3	2.64843	0.42271	2.08465	0.45215
0.5	2.86086	0.41332	2.15470	0.44806
0.7	3.17237	0.40085	2.24035	0.44324
1.0	4.10850	0.37023	2.41421	0.43404

Table 2 Selected values of α for Perfect gas

γ	β	α
1.2	11.00000	0.24828372
1.4	6.00000	0.32571203
1.6	4.33333	0.3779717
1.8	3.50000	0.41763534
2.0	3.00000	0.44948974

3.3 Numerical Solution of Flow Parameters

The numerical solution of the problem involves in applying Crout's reduction technique (Samuel D. Conte and Carl de Boor 1981) to evaluate the flow parameters such as density (G_{i+1}), velocity (U_{i+1}), pressure (Y_{i+1}), and radiation flux (J_{i+1}), from Eqs. (40-43) using MATLAB with a step size of $h = 10^{-4}$ and an error tolerance of 10 significant digits. The whole solution procedure is repeated until the shock conditions are satisfied within the said accuracy.

4. RESULTS AND DISCUSSIONS

In this paper, the entire computational work has been carried out using MATLAB. Numerical calculations are performed for the values of non-ideal parameters $\rho_0 = 1$, $R = 1$, $m = 3/2$, $n = -1/2$, $s = 1$, $q = 0$ and $\sigma = 1.42$. The similarity exponent α for various values of constant parameter b and fixed values of non-idealness parameter Γ_0 are listed in Tables 1 and 2. We observe from Table 1, decrease in the values of similarity exponent α and increase in the measure of shock strength β with increasing values of constant parameter b and for fixed values of non-idealness parameter Γ_0. Also from Table 2, for perfect gas case a reverse trend is observed in the values of similarity exponent α and measure of shock strength β for various values of adiabatic exponent γ. The variations of non-dimensional flow variables and radiation flux for the considered non-idealness parameters for both Royce and ideal gas EOSs are shown in Figs. 2-13.

It is observed from Figs. 2 and 3 that the flow variable density (for both cylindrical and spherical geometry) is high at the shock front (for the Royce EOS) reduces with the increase in the non-idealness parameters and reduce gradually as λ increases. It is observed that at the shock front discontinuity appeared in density profiles is subject to physical requirement that the radiation flux cannot change across it and the mean collision time of particles is proportional to the gas density.

Also from Figs. 4 and 5, it is observed for Royce EOS for the cylindrical and spherical geometries for different values of non-ideal parameters a sharp increase in velocity profiles for $\lambda = 1$ for a short range of λ and decrease steadily with the variation in λ. It is notable that increase in the non-idealness parameters (from Tables 1 and 2) have effect on β. As β value increases, increase in velocity, pressure is prominent for both the EOS. Thus it is observed from Fig. 3, that increase in β does not automatically decelerate the shock front but the velocity and pressure behind the shock front increases quickly in the presence of mono-chromatic radiation and decrease slowly and become constant. The variation in shock velocity causes the shock transition to expand to a scale larger than that of the system, so that the shock enters a different regime for real systems such as stellar atmosphere (Farnsworth and Clarke 1971). Hence the shock velocity will increase as cryogenic implosion performance improves allowing access to the radiative pressure regime.

The effect of non-idealness parameters (b) on the pressure distribution in the presence of fixed non-idealness parameter (Γ_0) is presented in Figs. 6 and 7.

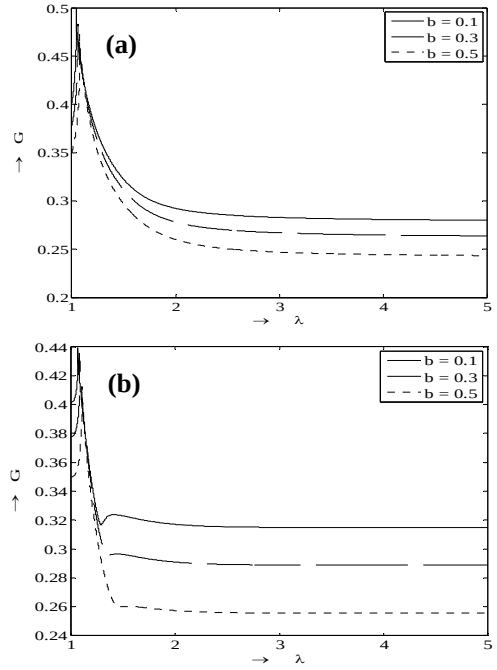

Fig. 2. Density profiles for Royce EOS when $\Gamma_0 = 1.4$, $\sigma = 1.42$; (a) $\Omega = 2$ and (b) $\Omega = 3$

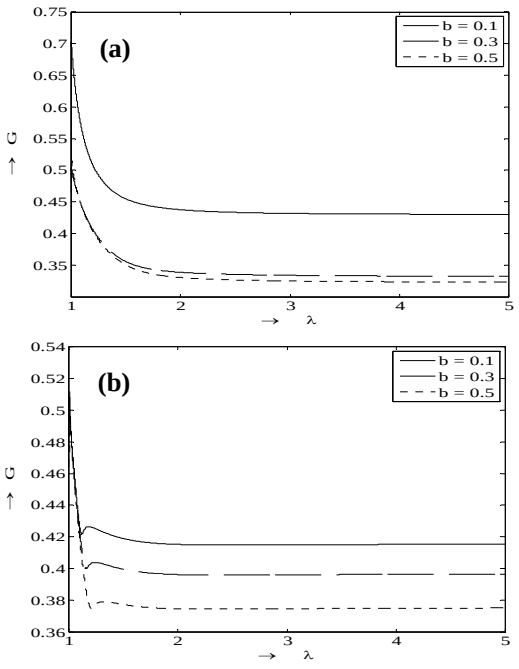

Fig. 3. Density profiles for Royce EOS when $\Gamma_0 = 2.0$, $\sigma = 1.42$; (a) $\Omega = 2$ and (b) $\Omega = 3$

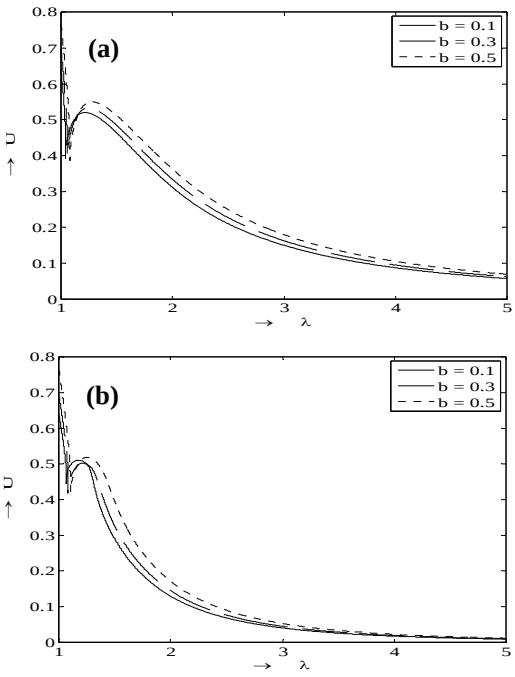

Fig. 4. Velocity profiles for Royce EOS when $\Gamma_0 = 1.4$, $\sigma = 1.42$; (a) $\Omega = 2$ and (b) $\Omega = 3$

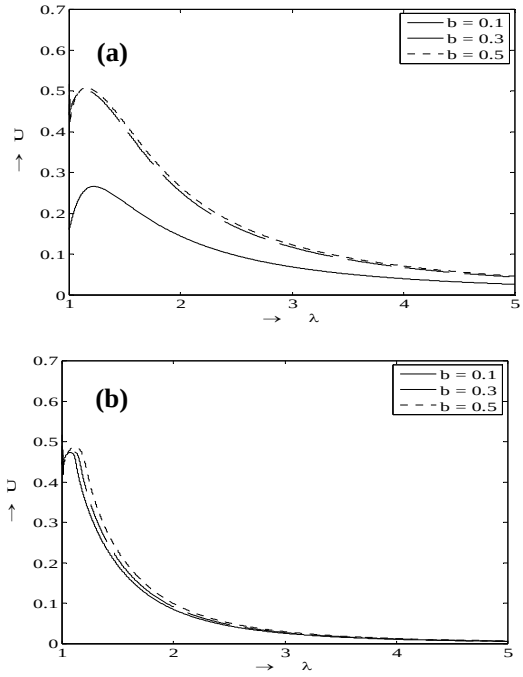

Fig. 5. Velocity profiles for Royce EOS when $\Gamma_0 = 2.0$, $\sigma = 1.42$; (a) $\Omega = 2$ and (b) $\Omega = 3$

The pressure distribution $Y(\lambda)$ increases as the constant parameter b increases. This is in agreement with physical fact that the velocity distribution increases with increasing b and also it is found that increase in pressure profiles has insignificant effect with increasing values of λ for both cases of geometry $\Omega = 2$, 3 and also the gas pressure decreases with increase in λ.

A similar trend is observed in the radiation profiles from Figs. 8 and 9.

The density, velocity, and pressure profiles for ideal gas equation of state are presented in Figs. 10-12 respectively for various values of γ. Figures 10(a) and 10(b) depict density profiles of both cylindrical, spherical geometry for different values

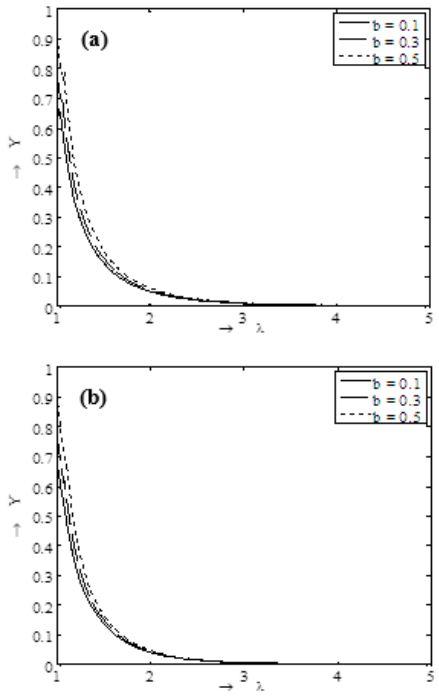

Fig. 6. Pressure profiles for Royce EOS when $\Gamma_0 = 1.4$, $\sigma = 1.42$; (a) $\Omega = 2$ and (b) $\Omega = 3$

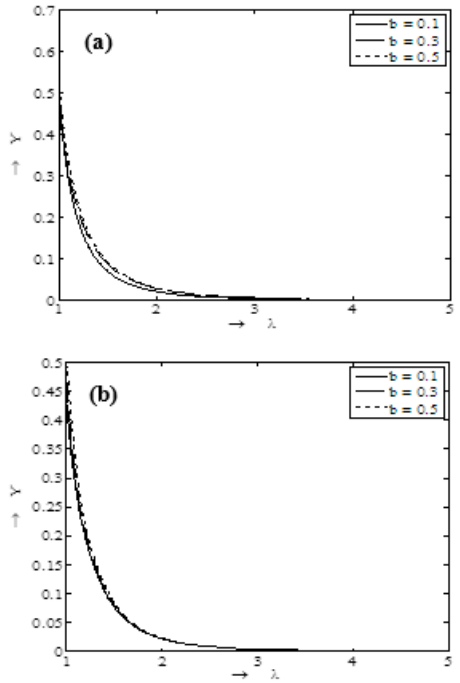

Fig. 7. Pressure profiles for Royce EOS when $\Gamma_0 = 2.0$, $\sigma = 1.42$; (a) $\Omega = 2$ and (b) $\Omega = 3$

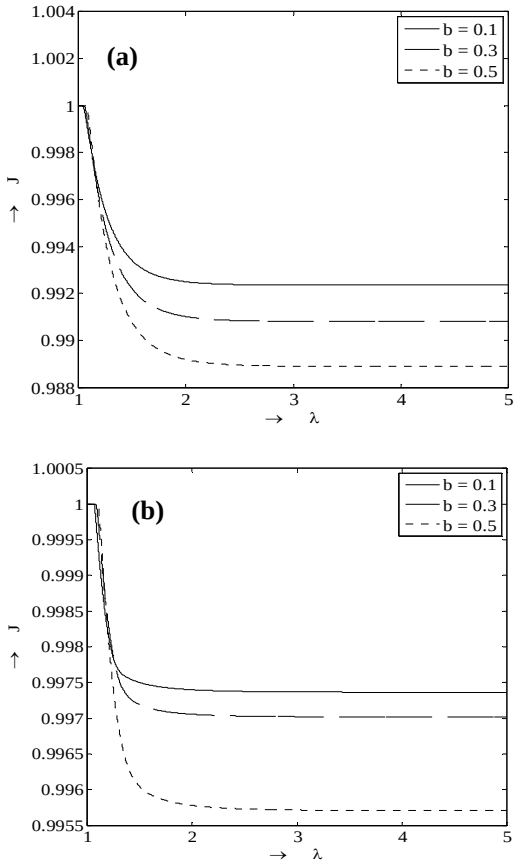

Fig. 8. Radiation profiles for Royce EOS when $\Gamma_0 = 1.4$, $\sigma = 1.42$; (a) $\Omega = 2$ and (b) $\Omega = 3$

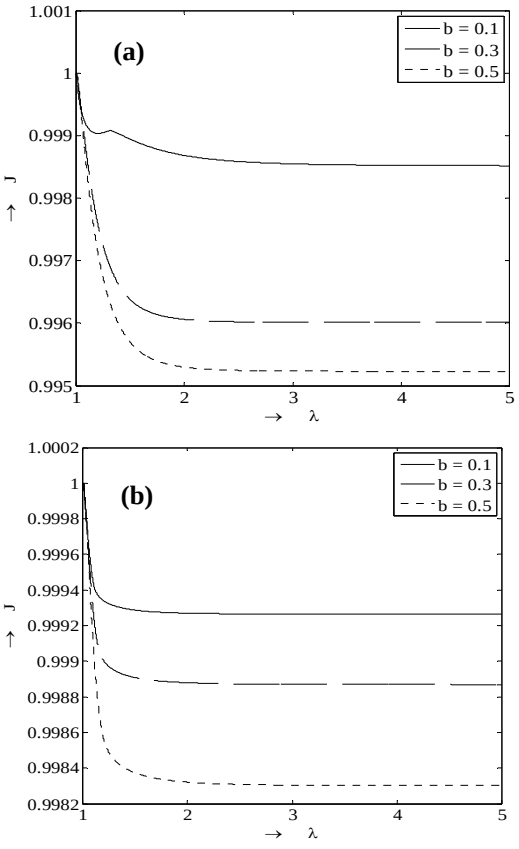

Fig. 9. Radiation profiles for Royce EOS when $\Gamma_0 = 2.0$, $\sigma = 1.42$; (a) $\Omega = 2$ and (b) $\Omega = 3$

of adiabatic index (γ) respectively. We observe from Fig. 10 that density distribution increases with the increase of γ and decreases in a short range of λ and a small increase is seen as a bounce and then reduces along the λ. The velocity profiles for different values of adiabatic index γ presented in Fig. 11. A sharp raise in the velocity profiles is observed initially and decrease rapidly along λ-axis for both cases of geometry $\Omega = 2$, 3 respectively. Moreover, this behavior is similar to the case of Royce EOS for fixed values of adiabatic index γ and non-idealness parameter (b) but it is just an opposite trend for different values of adiabatic index γ. Figures 12(a) and 12(b) represent pressure profiles versus λ, for various values of adiabatic index γ.

The radiation flux profiles for perfect gas are presented in Fig. 13. It is observed that initially no variation in radiation flux distribution but then it is more with an increasing values of λ. It is observed that effect of radiation from the volume of a gas becomes important at distances away from the initial point and it modifies the shock structure.

5. CONCLUSIONS

Similarity solutions for the governing partial differential equations (PDEs) of one-dimensional unsteady motion of strong converging spherical and cylindrical shock wave with the effect of radiation is developed. We studied the behavior of flow parameters such as density, velocity, pressure, and radiation flux for flow-field behind a strong converging cylindrical, spherical shock wave propagating through a non-ideal stellar medium in the presence of monochromatic radiation. The finite difference approximation method is employed in the solution process. The effects of various physical parameters such as non-idealness parameter (b), Gruneisen parameter (Γ_0), as well as the specific heat ratio (γ) and material property (σ) on the flow variables are shown graphically. It is observed that increase in measure of shock strength $\beta\left(\frac{\rho}{\rho_0}\right)$ has effect on the shock front i.e., the velocity and pressure behind the shock front increases quickly in the presence of the monochromatic radiation and decreases gradually. We conclude from the above investigation (i) at the shock front discontinuity appeared in density profiles is subject to physical requirement that the radiation flux cannot change across it and the mean collision time of particles is proportional to the gas density and (ii) that effect of radiation from the volume of a gas becomes important at distances away from the initial point and it modifies the shock structure.

ACKNOWLEDGEMENT

The authors acknowledge with thanks the financial and technical support provided by Department of Science and Technology, New Delhi, through Inspire fellowship (IF110071).

The authors would like to thank the referees for their valuable suggestions and comments that improved the representation substantially.

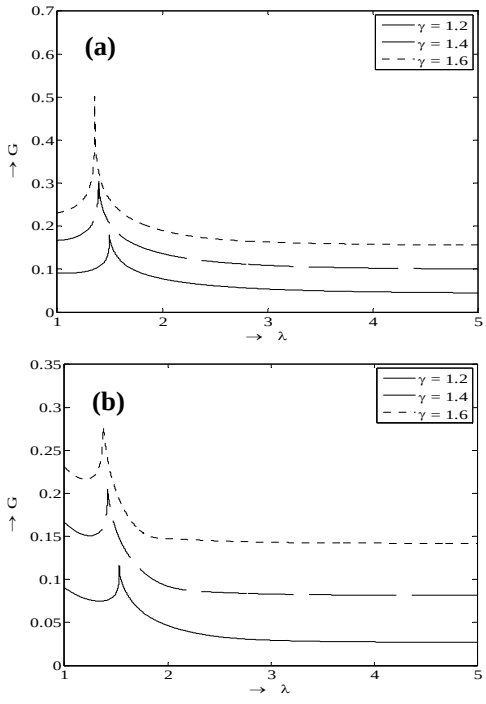

Fig. 10. Density profiles for perfect gas when $\sigma = \gamma$; (a) $\Omega = 2$ and (b) $\Omega = 3$

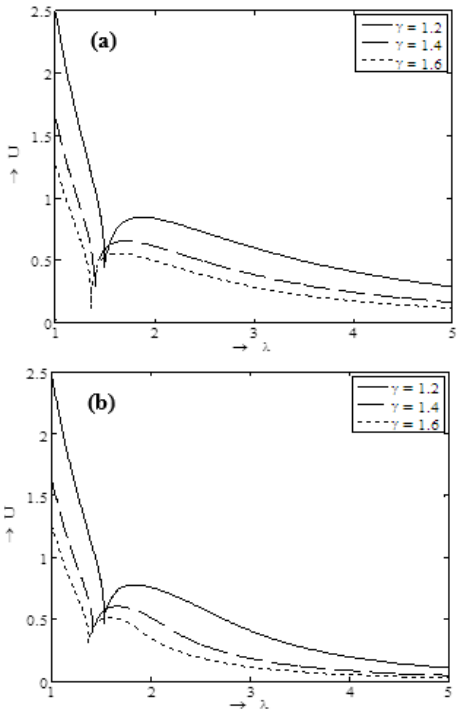

Fig. 11. Velocity profiles for perfect gas when $\sigma = \gamma$; (a) $\Omega = 2$ and (b) $\Omega = 3$

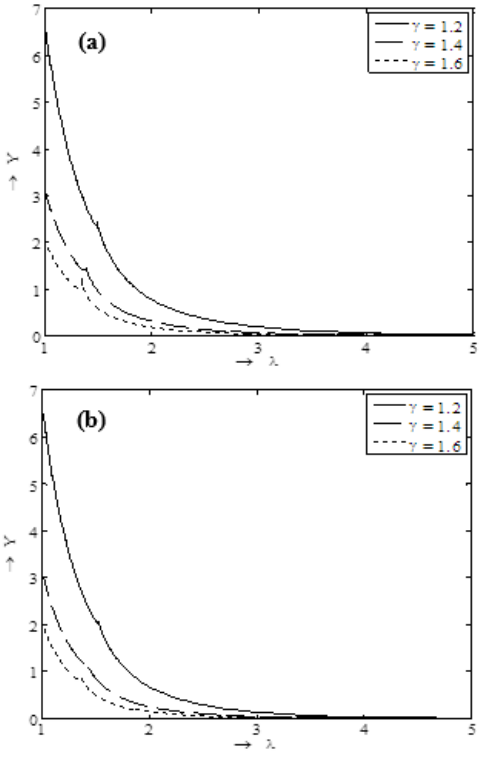

Fig. 12. Pressure profiles for perfect gas when $\sigma = \gamma$; (a) $\Omega = 2$ and (b) $\Omega = 3$

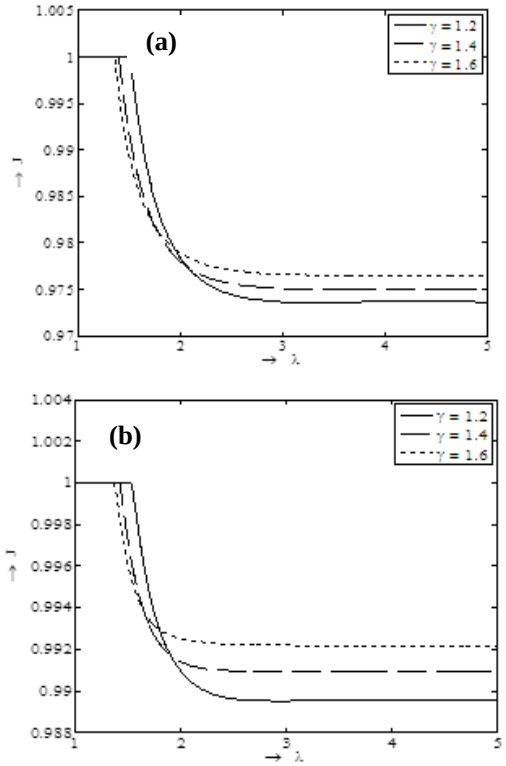

Fig. 13. Radiation profiles for perfect gas when $\sigma = \gamma$; (a) $\Omega = 2$ and (b) $\Omega = 3$

REFERENCES

Barnwal, S. P. and O. S. Srivastava (1983). Shock Waves in dusty gas with radiation effects. *Defence Science Journal* 33(1), 59-67.

Samuel D. Conte and Carl de Boor (1981). Elementary Numerical Analysis: An Algorithmic Appro- oach. I*nternational Series in Pure and App- lied Mathematics*, 3rd Edition, McGraw-Hill

Elliott, L. A. (1960). Similarity methods in radiation hydrodynamics. *Proceedings of the royal Society of London, Mathematical and Physical Sciences*, Ser. A 258(1294), 287-301.

Farnsworth, A. V. and J. H. Clarke (1971). Radiatively and collisionally structured Shock waves exhibiting large emission-convection ration *Physics of Fluids* 14(7), 1352-1360.

Flecks, B. and F. Scmitz (1993). On the interactions of hydrodynamic shock waves in stellar atmospheres. *Astronomy and Astrophysics* 273, 671-683.

Gail, H., M. Cuntz and P. Ulmschneider (1990). Wave pressure in stellar atmospheres due to shock wave trains. *Astronomy and Astro physics* 234(1-2), 359-365.

Ghoiem, A. F., M. M. Kamel, S. A. Berger and A. K. Oppenheim (1993) Effects of internal heat transfer on the structure of self-similar fluids 1(1), 24-29.

Gretler, W. and H. Steiner (1993). Blast wave in inhomogeneous atmospheres with counter pressure and heat transfer effects. *Shock waves* 3(2). 83-94.

Helliwell, J. B. (1969). Self-similar piston problems with radiative heat transfer. *Journals of fluid Mechanics* 37(3), 497-512.

Hirschler, T. and W. Gretler (2002). Similarity analysis of strong converging spherical shock waves in radiating gas. *Acta Mechanica* 154(1), 159-177.

Khudyakov, V. M. (1983). The self-similar problem of the motion of a gas under the action of monochromatic radiation. *Soviet Physics Doklady (trans. American institute of Physics)* 28(10), 853-855.

Leygnac, S., L. Boireau, C. Michaut, T. Lanz, C. Stehle, C. Clique and S. Bouquet (2006) Modelling multidimensional effects inpropagation of radiative shocks. *Physics of plasmas* 13(11), 113301(1-10).

Marshak, R. E. (1958).Effect of radiation on shock wave behaviour. *Physics of Fluids* 1(1), 24-29.

Narsimhulu, D., A. Ramu and D. K. Satpathi (2013). Similar Solution to shock waves in non-ideal magnetogasdynamics. *11th* International conference of Numerical Analysis and Applied

Mathematics, AIP conf., *Proc.,* 1558, 860-864.

Narsimhulu, D., A. Ramu and D. K. Satpathi (2016). Similarity solution of spherical shock wave-effect of Viscosity. Proyecciones *Journal of Mathematics* 35(1), 11-31.

NiCastro, J. R. A. J. (1970) Similarity analysis of the radiative gas dynamic equations with spherical symmetry. *Physics of Fluids* 13(8), 2000-2006.

Ramu, A. and M. P. Ranga Rao (1993). Converging spherical and cylindrical shock waves.*Journalof Engineering Mathematics* 27(4), 411-417.

Ramu, A., D. Narsimhulu and D. K. Satpathi (2014) Numerical study of shock waves in non-ideal magnetogasdynamics (MHD). *Journal of Egyptian Mathematical Society* 24(1), 116-124.

Sampaio, O. P. (2013). Radiation from a D-dimensional collision of shock waves: Numerical Methods. *International Journal of Modern Physics A* 28(22 & 23), 1340019 (1-37).

Sedov, L. I. (1982). Similarity and Dimensional Methods in Mechanics, Mir Publishers, USSR.

Taylor, K. L. and G. M. Ryan (2013). New self-similar radiation-hydrodynamics. Solutionin the high- energy density, equilibrium diffusion limit. *New Journal of Physics* 15(9), 095013(1-17).

Zedan, H. A. (2002). Applications of the group equations of the one-dimensional motion of gas under the influence of monochro- matic radiation. *Applied Mathematics and Computation* 132(1), 63-71.

Zel'dovich, Ya. B and Yu. P. Raizer (1967). *Physics of Shock Waves and High temperature Hydro- dynamic Phenomena*. New York: Academic Press